Multiple regulation by calcium of murine homologues of transient receptor potential proteins TRPC6 and TRPC7 expressed in HEK293 cells

Juan Shi[1,4], Emiko Mori[2], Yasuo Mori[2], Masayuki Mori[3], Jishuo Li[4], Yushi Ito[1] and Ryuji Inoue[1]

[1]*Department of Pharmacology, Graduate School of Medical Sciences, Kyushu University, Fukuoka 812–8582, Japan*
[2]*Laboratory of Molecular Biology, Department of Synthetic Chemistry and Biological Chemistry, Graduate School of Engineering, Kyoto University, Kyoto 606–8510, Japan*
[3]*National Institute for Physiological Sciences, Okazaki 444–8585, Aichi, Japan*
[4]*Department of Anatomy, the Fourth Military Medical University, Xi'an 710032, China*

We investigated, by using the patch clamp technique, Ca^{2+}-mediated regulation of heterologously expressed TRPC6 and TRPC7 proteins in HEK293 cells, two closely related homologues of the transient receptor potential (TRP) family and molecular candidates for native receptor-operated Ca^{2+} entry channels. With nystatin-perforated recording, the magnitude and time courses of activation and inactivation of carbachol (CCh; 100 μM)-activated TRPC6 currents (I_{TRPC6}) were enhanced and accelerated, respectively, by extracellular Ca^{2+} (Ca_o^{2+}) whether it was continuously present or applied after receptor stimulation. In contrast, Ca_o^{2+} solely inhibited TRPC7 currents (I_{TRPC7}). Vigorous buffering of intracellular Ca^{2+} (Ca_i^{2+}) under conventional whole-cell clamp abolished the slow potentiating (i.e. accelerated activation) and inactivating effects of Ca_o^{2+}, disclosing fast potentiation (EC_{50}: ∼0.4 mM) and inhibition (IC_{50}: ∼4 mM) of I_{TRPC6} and fast inhibition (IC_{50}: ∼0.4 mM) of I_{TRPC7}. This inhibition of I_{TRPC6} and I_{TRPC7} seems to be associated with voltage-dependent reductions of unitary conductance and open probability at the single channel level, whereas the potentiation of I_{TRPC6} showed little voltage dependence and was mimicked by Sr^{2+} but not Ba^{2+}. The activation process of I_{TRPC6} or its acceleration by Ca_o^{2+} probably involves phosphorylation by calmodulin (CaM)-dependent kinase II (CaMKII), as pretreatment with calmidazolium (3 μM), coexpression of Ca^{2+} -insesentive mutant CaM, and intracellular perfusion of the non-hydrolysable ATP analogue AMP-PNP and a CaMKII-specific inhibitory peptide all effectively prevented channel activation. However, this was not observed for TRPC7. Instead, single CCh-activated TRPC7 channel activity was concentration-dependently suppressed by nanomolar Ca_i^{2+} via CaM and conversely enhanced by IP_3. In addition, the inactivation time course of I_{TRPC6} was significantly retarded by pharmacological inhibition of protein kinase C (PKC). These results collectively suggest that TRPC6 and 7 channels are multiply regulated by Ca^{2+} from both sides of the membrane through differential Ca^{2+}—CaM-dependent and -independent mechanisms.

(Resubmitted 2 September 2004; accepted after revision 1 October 2004; first published online 7 October 2004)
Corresponding author R. Inoue: Department of Pharmacology, Graduate School of Medical Sciences, Kyushu University, Fukuoka 812–8582, Japan. Email: inouery@pharmaco.med.kyushu-u.ac.jp

Ca^{2+}-dependent regulation is a ubiquitous mechanism by which the activity of various types of Ca^{2+}-permeable cation channels is finely tuned (Levitan, 1999; Saimi & Kung, 2002). Examples are not restricted to small conductance Ca^{2+}-activated K^+ channels, cyclic nucleotide-gated cation channel, NMDA receptor, ryanodine/inositol 1,4,5,-trisphospate (IP_3) receptors, and L- and P/Q-type voltage-dependent Ca^{2+} channels, but also include a variety of native receptor-operated cation (ROC) channels with less well elucidated properties (e.g. Siemen, 1993) and their molecular candidates, the mammalian homologues of *Drosophila* transient receptor potential (TRP/TRPL) protein (Montell, 2001; Clapham *et al.* 2001; Minke & Cook, 2002).

In photoreceptor cells of the wild-type *Drosophila*'s eye, it was originally found that light-induced currents which reflect the opening of TRP and TRPL channels are dually modulated by photolytically released Ca^{2+}

 DOI: 10.1113/jphysiol.2004.075051

with facilitation and inactivation in rising and plateau phases of the response, respectively (Hardie, 1995). Later, a similar reciprocal regulation by Ca^{2+} was also found for the canonical members of the TRP superfamily (TRPC). Earlier studies demonstrated that manoeuvres to increase Ca_i^{2+} concentration ($[Ca^{2+}]_i$) such as application of ionomycin and direct Ca^{2+} infusion into the cell enhanced the activity of heterologously expressed TRPC3 channels (Zitt *et al.* 1997), while sustained elevation in $[Ca^{2+}]_i$ by use of Ca^{2+}/EGTA or BAPTA failed to stimulate or even inhibited them (Zitt *et al.* 1997; Kamouchi *et al.* 1999). It has subsequently been shown that a CaM binding site (CIRB), which also exhibits binding affinity for the IP_3 receptor (IP_3R), is present on the carboxy tail of TRPC3 channels (Zhang *et al.* 2001), and CaM binding sites highly homologous to this are identified in all other members of the TRPC family (Tang *et al.* 2001). It has experimentally been shown that application of CaM antagonists or IP_3R peptides relieves the tonic inhibitory effects of CaM via CIRB thereby increasing the basal TRPC3 channel activity. This observation has been interpreted to represent the molecular mechanism underlying store depletion-activated Ca^{2+} entry (SOC) during receptor stimulation (Kiselyov *et al.* 1998; Boulay *et al.* 1999; Zhang *et al.* 2001). However, there is also good evidence to suggest that members of the TRPC3/6/7 subfamily are activated by diacylglycerol in a store-independent fashion (e.g. Hofmann *et al.* 1999; Trebak *et al.* 2003). Inhibitory actions of CaM have also been suggested for TRPC4 (Tang *et al.* 2001) and TRPC1 (Singh *et al.* 2002; Vaca & Sampieri, 2002). In the latter, the role of CaM has been assigned to Ca^{2+}-dependent feedback inhibition of endogenous SOC via a C-terminal site more distal to CIRB (Singh *et al.* 2002) as well as prolongation of delay of SOC activation via a common binding site for CaM and IP_3R, mostly likely CIRB (Vaca & Sampieri, 2002). As for other TRPC members, both spontaneous and agonist-induced activities of the TRPC5 channel have been shown to be enhanced by Ca^{2+} entering through the channel itself (Okada *et al.* 1998; Yamada *et al.* 2000), which are also potentiated directly by extracellular Ca^{2+} (and lanthanides; Jung *et al.* 2003), as has been found in several native ROC channels (e.g. Inoue, 1991; Helliwell & Large, 1998; Aromolaran & Large, 1999). Furthermore, preliminary results have indicated that the magnitude of agonist-induced TRPC6 currents dramatically changes in response to extracellularly applied Ca^{2+} with a complex time course (Inoue *et al.* 2001). These findings strongly suggest that Ca^{2+}-mediated regulation from both sides of the cell membrane may be a powerful and common means to modulate TRPC channel activity.

There is now a growing body of evidence that TRPC6 is broadly distributed in extra-brain tissues, especially enriched in vascular smooth muscles, and may function as an integral subunit of native ROC channels activated via sympathetic nerve excitation, intravascular pressure increase and vasoactive peptides and growth hormones (Inoue *et al.* 2001, 2004; Jung *et al.* 2002; Welsh *et al.* 2002). Despite this potential importance, little detailed information is yet available as to how Ca^{2+} modulates TRPC6 channel activity, although a recent Ca^{2+} fluorometric study has reported that a CaM-mediated mechanism is involved in the positive modulation of this channel (Boulay, 2002). The present study was thus initiated to gain more insight for the complex actions of extra- and intracellular Ca^{2+} on TRPC6 channels in comparison with TRPC7, another member of the same subfamily which exhibits contrasting responses to Ca^{2+}, in terms of whole-cell and single channel recordings. As the results, we have found that TRPC6 and TRPC7 channels undergo effective but differential regulation by extra- and intracellular Ca^{2+} in CaM-dependent and -independent manners. Part of this study has been communicated to the 76th annual meeting of the Japanese Pharmacological Society (Shi *et al.* 2003).

Methods

Cell culture and transfection

Human embryonic kidney 293 (HEK293) cells were maintained in Dulbecco's modified Eagle's medium (DMEM) supplemented with 10% fetal bovine serum. For transfection, the cells were reseeded in a 35 mm culture dish and allowed to grow to 40–60% confluency, and then transfected with a mixture of 2 μg plasmid vector (pCI-neo) incorporating TRPC DNAs (murine TRPC6, murine TRPC7 or their six chimeras; see below) and 0.4 μg pCI-neo-πH3-CD8 (cDNA of the T-cell antigen CD8), with the aid of 20 μl of the transfection reagent SuperFect™ (Qiagen, Germany). In some experiments, 2 μg of plasmid DNA for mutant calmodulin (mutCaM; see below) was cotransfected. About 24 h after transfection, cells were reseeded onto coverslips pre-coated with 100 μM poly-L-lysine. Electrophysiological measurements were performed within 48–72 h after transfection.

Construction of TRPC6/7 chimeras and mutant calmodulin (mutCaM)

The TRPC6/7 chimeras and the calmodulin mutant (mutCaM) were constructed by using PCR. In T667, the amino acid sequence 1–726 containing the N-terminus (1–402) and the hydrophobic core H1–H8 (403–726) of murine TRPC6 (Mori *et al.* 1998) was linked to the C-terminal sequence 673–862 of murine TRPC7 (Okada *et al.* 1999). In T776, the TRPC7 sequence 1–672 containing the N-terminus (1–348) and H1–H8 (349–672) was linked to the TRPC6 C-terminus 727–930. For the design of other chimeras, see Supplementary Fig. 1.

In mutCaM, aspartate residues 21, 57, 94 and 130 in 4 E-F hands were replaced with alanine to ablate the Ca^{2+}-binding ability of calmodulin.

Electrophysiology

The details of the three variants of the patch clamp technique employed in this study (i.e. nystatin-perforated, conventional whole-cell, and single channel recordings) are essentially the same as described elsewhere (see supplementary information in Inoue *et al.* 2001). Leak currents were estimated by constructing the current–voltage relationship in non-transfected cells. However, in successful recordings, the leak current estimated in this way was as small as 0.14 ± 0.05 pA pF^{-1} at -60 mV ($n = 15$), and thus not corrected in the present study. For single channel recordings, pipette electrodes having a resistance of 5–10, 4–5 and 1.5–2 MΩ (with pipette solution described below) were used in cell-attached (C/A), outside-out (O/O) and inside-out (I/O) configurations, respectively, while for whole-cell recordings, the pipette input resistance was 2.5–4 MΩ. Voltage generation and current signal acquisition were implemented through a high-impedance low-noise patch clamp amplifier (EPC9; HEKA Elektronik, Germany). Sampled data were low-pass filtered at 1 kHz (I/O, O/O) or 2 kHz (C/A) and stored on a computer hard disc after digitization at 2–5 kHz (I/O, O/O) or 20 kHz (C/A). Long-term recordings (> 30 s, e.g. whole-cell currents in Fig. 1) were performed in conjunction with an A/D, D/A converter, Powerlab/400 (ADInstruments, Australia; sampling rate: 100 Hz), and data evaluation was made with the associated software, Chart v3.6. Concentration–response relationships were fitted by a non-linear least square routine, using two types of Hill equation. For single Hill fitting:

$$I = 1.0/[1 + (C/\mathrm{IC}_{50})^n]$$

where I, C, IC_{50}, and n denote the normalized current amplitude (the ratio of currents after to before drug application), drug concentration, half-maximal inhibitory concentration and the cooperativity factor, respectively.

For double Hill fitting (Fig. 2):

$$I = [1 + \Delta I/[1 + (\mathrm{EC}_{50}/C)^{n'}]/[1 + (C/\mathrm{IC}_{50})^n]$$

where I, C, IC_{50}, and n have the same meaning as described above, while ΔI, EC_{50} and n' denote the normalized current increase, half-maximal effective concentration and the cooperativity factor, respectively. It should, however, be mentioned that the fitting using this equation could provide only approximate values for EC_{50} and IC_{50}, since the results of double non-linear fitting were prone to small changes in data points of a limited number.

Single channel analysis was made using the software Pulsefit and/or a freely distributed web software Win/EDR v.2.3 (Dr J. Dempster, University of Strathclyde, UK). To evaluate the unitary current amplitude, all-points or all-points-in-open-state amplitude histograms were constructed. To calculate the relative open probability (NP_o), single channel currents were averaged for each 3–5 s time interval and then converted to the NP_o value according to $I = iNP_o$ where I, i, N and P_o denote the averaged single channel current, unitary amplitude, the number of open channels and their open probability, respectively. The baseline for channel opening was normally determined by constructing all-point histograms, but when this was unfeasible due to baseline drifts, the records were divided into several segments, each of which was corrected for its linear trend by visual inspection. In the case of large I/O or O/O patch experiments where precise evaluation of unitary amplitude (i) was often difficult due to multiple channel openings, we adopted the averaged 'i' value determined by C/A recordings.

Solutions

Solutions with the following composition were used. Pipette solution for nystatin-perforated recording (mM): 140 CsCl, 2 $MgCl_2$, 10 Hepes, 10 glucose (adjusted to pH 7.2 with Tris base). Internal solution for conventional whole-cell recording and O/O recording (mM): 120 CsOH, 120 aspartate, 20 CsCl, 2 $MgCl_2$, 10 BAPTA, 4 $CaCl_2$, 10 Hepes, 2 ATP, 0.1 GTP, 10 glucose (adjusted to pH 7.2 with Tris base; $[Ca^{2+}] = ca$ 80 nM; '10 BAPTA/4 Ca internal solution'). In some experiments in which the effects of a broader range of $[Ca^{2+}]_i$ were investigated (e.g. Figs 5*A* and 6*A*), $[Ca^{2+}]$ was adjusted by using 10 mM BAPTA and appropriate concentrations of Ca^{2+} as performed in I/O recordings (see below). In Figs 8 and 9, in order to only weakly buffer $[Ca^{2+}]_i$, 10 mM BAPTA was replaced by 0.1 mM EGTA and 0.04 mM Ca^{2+} added; adjusted to pH 7.2 with Tris base; '0.1 EGTA-internal solution'). Ca^{2+}-free external solution (mM): 140 NaCl, 5 KCl, 1.2 $MgCl_2$, 1 EGTA, 10 Hepes, 10 glucose (pH 7.4, adjusted with Tris base). For Ca^{2+}-, Sr^{2+}-, or Ba^{2+}-containing external solutions, various concentrations of $CaCl_2$, $SrCl_2$ or $BaCl_2$ were added to the Ca^{2+}-free solution with the omission of EGTA. Unless otherwise stated, pipette solution for C/A and I/O recordings contained (mM): 140 NaCl, 5 tetraethylammonium-Cl, 1.2 $MgCl_2$, 0.1 $CaCl_2$, 10 Hepes, 10 glucose, 0.1 carbacol (CCh) (pH 7.4, adjusted with Tris base). Ca^{2+} at 0.1 mM was usually necessary to successfully obtain the 'giga' seal. For C/A recording, cells were bathed in high potassium solution with the following composition to null the transmembrane potential (mM): 140 KCl, 2 EGTA, 2 $MgCl_2$, 10 Hepes (pH 7.2, adjusted with Tris base). The bathing solution for I/O recording

had the composition (mM): 120 CsOH, 120 aspartate, 20 CsCl, 2 $MgSO_4$, 2 EGTA, 10 Hepes, 2 ATP, 0.1 GTP (pH 7.2, adjusted with Tris base). To obtain the micromolar range $[Ca^{2+}]$, a low affinity buffer, HEDTA, rather than EGTA was used. The amount of Ca^{2+} required to obtain the desired $[Ca^{2+}]$ was calculated using Fabiato and Fabiato's program with enthalpic and ionic strength corrections (Brooks & Storey, 1992), as performed previously (Inoue & Ito, 2000).

In whole-cell, O/O and I/O single channel recordings, solutions were rapidly applied through a solenoid-driven fast solution change device 'Y-tube' (Inoue *et al.* 2001).

Chemicals

Calmidazolium (chloride salt), 1-oleoyl-2-acetyl-sn-glycerol (OAG), 5′-adenylylimidodiphosphate (AMP-PNP), GTPγS, calmodulin, KN-62, okadaic acid, FK506, CaM-kinase II inhibitory peptide (CAMK-$IP_{(281–309)}$), myosin light chain kinase (MLCK) inhibitory peptide (MLCK-$IP_{(480–501)}$), and protein kinase C inhibitory peptide (PKC-$IP_{(19–36)}$) were purchased from Calbiochem (La Jolla, CA, USA), carbachol, Hepes, $SrCl_2$, $BaCl_2$ and PDBu from Sigma (St Louis, MO, USA), ATP, GTP, BAPTA and EGTA from Dojindo (Kumamoto, Japan), and MLCK inhibitory peptide ($MLCK_{(11–19)}$ amide) from Alexis (Nottingham, UK). HEDTA was kindly provided by BASF Japan, Ltd.

Statistics

All data are expressed as means ± S.E.M. To evaluate statistical significance of the difference between a given set of data, Student's paired and unpaired *t* test, and one-way ANOVA with pooled variance *t* test (Bonferroni's correction) were employed for single and multiple comparisons, respectively.

Results

Multiple effects of Ca^{2+} on heterologously expressed TRPC6 currents

Under quasi-physiological conditions with nystatin-perforated voltage-clamp (Horn & Marty, 1988; −60 mV), human embryonic kidney 293 (HEK293) cells expressing murine TRPC6 differentially responded to muscarinic receptor stimulation (carbachol; CCh 100 μM) at different levels of external Ca^{2+} (Ca^{2+}_o) (Fig. 1*A*). The time courses of activation and inactivation of CCh-induced current (I_{TRPC6}) evaluated in the same cell were clearly faster in the presence of 1 mM Ca^{2+}_o as compared with its absence. Paired data from 12 cells indicate that three parameters representing the rates of activation and inactivation, t_{10}, $t_{10–90}$ and $t_{90–50}$, are significantly shorter in the presence of Ca^{2+}_o (Fig. 1*B*). The extent of maximum activation (i.e. peak amplitude) was also greater with 1 mM Ca^{2+} in the bath (25.7 ± 2.8 *versus* 37.8 ± 4.9 pA pF^{-1} at −60 mV, $n = 12$; $P < 0.05$ with paired *t* test). These results show that the presence of Ca^{2+}_o enhances the extent of activation and accelerates the activation and inactivation processes of I_{TRPC6}. Similar enhancement and acceleration of activation (or potentiation) and of inactivation were observed, when Ca^{2+}_o was added after I_{TRPC6} had already reached the peak activation (Fig. 1*C*). In this case, however, in addition to slower potentiating and inactivating phases (#), an immediate increase in I_{TRPC6} amplitude (*–*), which was not discernible in the continued presence of Ca^{2+}_o (Fig. 1*A*), was also visualized.

The potentiating and inactivating effects of Ca^{2+}_o on I_{TRPC6} were still observed when conventional whole-cell recording with weak Ca^{2+} buffering capacity (0.1 EGTA internal solution) was used (data not shown). However, inclusion of 10 mM BAPTA in the pipette (10 BAPTA/4 Ca internal solution; calculated $[Ca^{2+}]_i = 80$ nM; conventional whole-cell clamp mode) selectively abolished the slow potentiating and inactivating effects of Ca^{2+}_o on I_{TRPC6} without affecting the fast potentiating actions (Fig. 1*D* and *E*), suggesting that the slow effects of Ca^{2+}_o are mediated by elevation in $[Ca^{2+}]_i$. Under these conditions, the effects of Ca^{2+}_o on I_{TRPC6} occurred as a biphasic function of $[Ca^{2+}]_o$ characterized by potentiation in the submilli- to millimolar range (< 1–3 mM; apparent EC_{50}: ∼0.4 mM) and inhibition in a higher concentration range (> 1–3 mM; apparent IC_{50}: ∼4 mM) (Fig. 2*A* and *C*). These Ca^{2+}_o effects most likely result from the actions on TRPC6 channel *per se*, since comparable $[Ca^{2+}]_o$ dependence was observed when I_{TRPC6} was more directly activated by GTPγS or OAG, by bypassing the receptor, G-protein or phospholipase C (PLC) (Fig. 2*B* and *C*). Similar biphasic (but less pronounced) effects on I_{TRPC6} were also observed for Sr^{2+}, but were virtually absent for another Ca^{2+}-mimetic, Ba^{2+} (Fig. 2*D–F*).

The rapidity and resistance to vigorous $[Ca^{2+}]_i$ buffering of fast potentiation and inhibition by Ca^{2+} and Sr^{2+} suggest that their site(s) of actions may reside at the extracellular side of the TRPC6 channel. In strong support of this idea, the extent of potentiation and inhibition were not changed by clamping $[Ca^{2+}]_i$ to a more elevated level (2 μM; filled circles in Fig. 2*C*), and quantitatively comparable effects of Ca^{2+}_o could still be obtained on single TRPC6 channel activity recorded in the cell-free, outside-out (O/O) patch configuration (Fig. 3*A* and *B*).

The current–voltage (*I–V*) relationships for macroscopic I_{TRPC6} show that the fast inhibition by high millimolar Ca^{2+}_o occurs via a voltage-dependent mechanism; the extent of the inhibition was significantly decreased at strongly depolarized membrane potentials (dotted *versus* thin continuous curves in Fig. 3*C*; percentage inhibition by 10 mM Ca^{2+}_o relative to 0 mM: $75 \pm 5\%$ at −100 mV, $42 \pm 6\%$ at 100 mV, $n = 7$;

$P < 0.05$). This voltage dependence can be accounted for at least in part by voltage-dependent reductions of the unitary conductance and degree of activation (NP_o) of single TRPC6 channels, since both reductions were relieved at strongly depolarized potentials (Fig. 3*D*; open triangles in Fig. 3*E* and *F*). In contrast, the fast potentiation of I_{TRPC6} at sub- to low millimolar Ca_o^{2+} exhibited little sign of voltage dependence, as evidenced by an

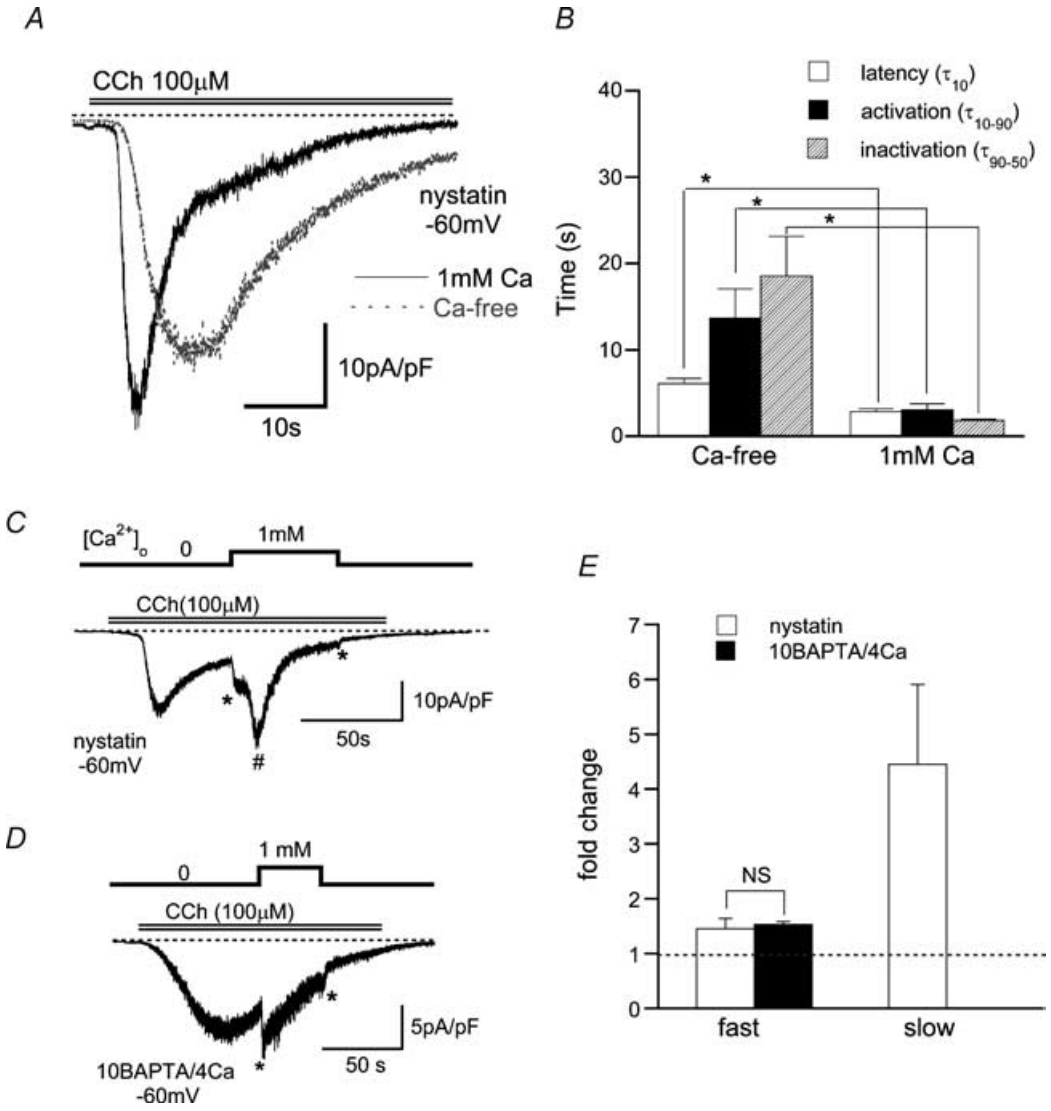

Figure 1. Acceleration of activation and inactivation time courses of murine TRPC6 currents by extracellular Ca^{2+} (Ca_o^{2+})

Holding potential: −60 mV. *A*, typical traces for CCh (100 μM)-evoked TRPC6 currents (I_{TRPC6}) in the presence (black, continuous line) and absence (grey, dotted line) of 1 mM Ca^{2+} in the bath, recorded from the same cell with nystatin-perforated recording. *B*, summary of latency (τ_{10}; time for 10% activation of the peak from the onset of CCh application), activation time (τ_{10-90}; time for 10–90% activation of the peak), and inactivation time (τ_{90-50}; time for 90–50% of the peak in inactivation phase) of I_{TRPC6} with 0 and 1 mM Ca^{2+} evaluated from the experiments as shown in *A* ($n = 12$). Repeated application of CCh at short intervals (< 5min) usually resulted in a rundown and slowed activation and deactivation of I_{TRPC6}. To minimize the errors arising from this problem, I_{TRPC6} was activated at an interval of 10 min, which led to recovery of the second response to CCh to 0.82 ± 0.09 of the first one ($n = 9$; evaluated in Ca^{2+}-free external solution), and the response in the presence of Ca_o^{2+} was taken on the second application of CCh. *C* and *D*, I_{TRPC6} was first activated in the absence of Ca_o^{2+} and then exposed to 1 mM Ca_o^{2+}, under nystatin-perforated and conventional whole-cell (10 BAPTA/4 Ca internal solution) voltage clamp, respectively. *E*; summary of the effects of Ca_o^{2+} (1 mM) on I_{TRPC6} such as illustrated in *C* and *D*. Relative I_{TRPC6} amplitude (fold change) is calculated as the ratio of I_{TRPC6} amplitude just after to that before (no Ca^{2+} present) application of Ca_o^{2+}. For slow Ca_o^{2+}-induced potentiation (#), I_{TRPC6} amplitude at the peak potentiation was normalized to that just before application of Ca_o^{2+}. Symbols '*–*' and '#' stand for the fast potentiation and slow potentiation, respectively. $n = 5$–8. '*' in *B*; $P < 0.05$ with paired *t* test. 'NS' in *E* denotes no statistical significance.

almost symmetrically increased *I–V* relationship (dotted *versus* thick continuous curves in Fig. 3*C*) and unaltered unitary amplitude or NP_o values at different potentials (filled circles in Fig. 3*E* and *F*). These results suggest that the mechanism underlying the potentiation may be different from that for the inhibition, but in the present study, we could not unequivocally figure out what changes in single channel properties contribute to the former.

Ca_o^{2+} inhibits TRPC7 channels

TRPC7 is a closest homologue of TRPC6 and has been shown to exhibit much higher spontaneous activity than TRPC6 and undergo inhibitory actions of Ca_o^{2+} (Okada *et al.* 1999). As demonstrated in Fig. 4, over a broad range of $[Ca^{2+}]_o$, Ca_o^{2+} merely caused a concentration-dependent inhibition of currents due to TRPC7 expression (spontaneous plus CCh-induced currents; I_{TRPC7}), irrespective of the species of activators

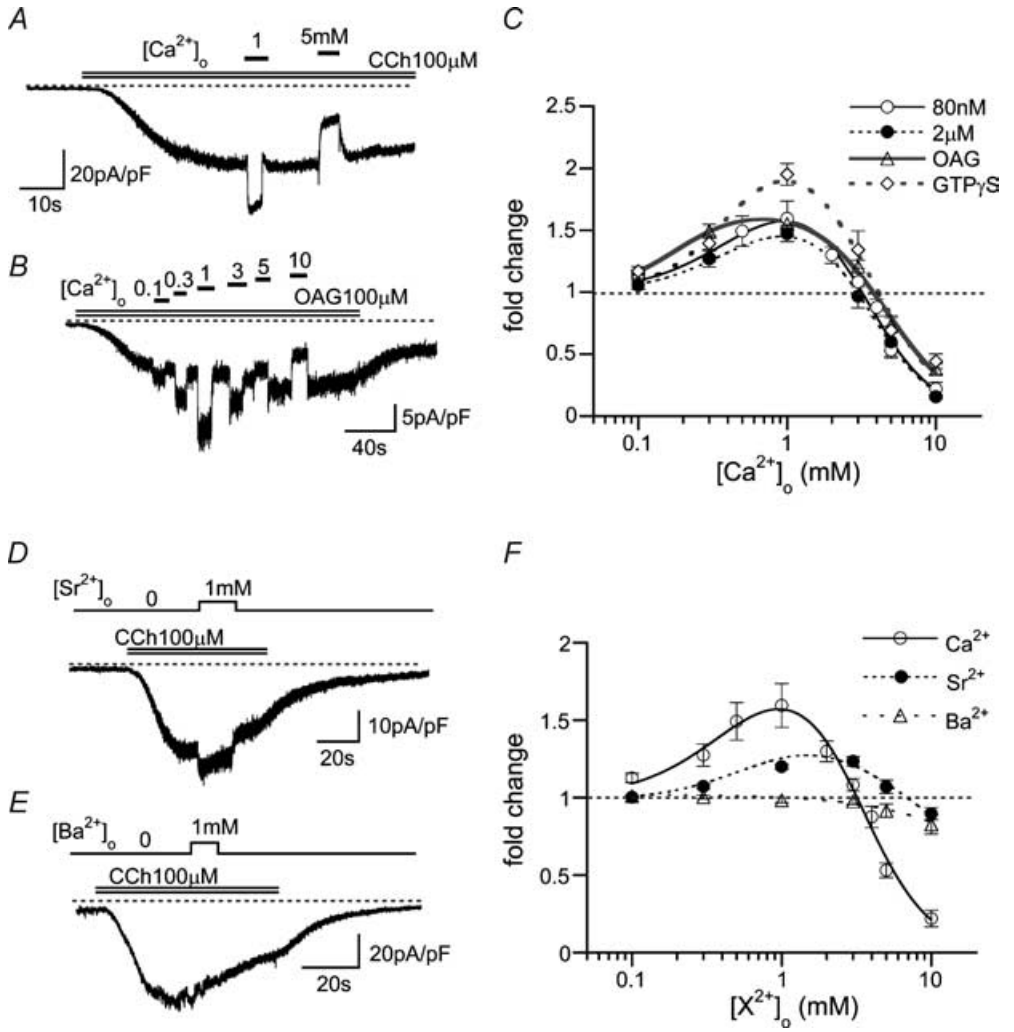

Figure 2. Biphasic effects of Ca_o^{2+} on I_{TRPC6} under strongly intracellular Ca^{2+} (Ca_i^{2+})-buffering conditions
Recording conditions used were the same as in Fig. 1*D*. *A* and *B*, typical examples of I_{TRPC6} at varying $[Ca^{2+}]_o$ evoked by 100 μM CCh (*A*) or OAG (*B*). *C*, relationships between $[Ca^{2+}]_o$ and relative I_{TRPC6} amplitude (fold change) under various conditions; 100 μM CCh with $[Ca^{2+}]_i = 80$ nM (10 mM BAPTA/4 mM Ca^{2+}, open circles) or 2 μM (10 mM BAPTA/9.5 mM Ca^{2+}, filled circles); 100 μM OAG ($[Ca^{2+}]_i$: 80 nM, open triangles); 100 μM GTPγS ($[Ca^{2+}]_i$: 80 nM, open diamonds). $n = 5$–12. *D* and *E*, typical examples of the effects of 1 mM extracellular Sr^{2+} (*D*) and Ba^{2+} (*E*) on I_{TRPC6} evoked by 100 μM CCh ($[Ca^{2+}]_i$: 80 nM). *F*; relationships between relative I_{TRPC6} amplitude (fold change) and extracellular Ca^{2+}, Sr^{2+} or Ba^{2+} concentration. $n = 5$–14. Curves in *C* and *F* are drawn according to the results of double Hill fitting (see Methods), which gave the EC_{50} and IC_{50} values (mM), respectively, in *C* of 0.44 and 3.56 (80 nM), 0.42 and 3.61 (2 μM), 0.38 and 4.27 (OAG), and 0.41 and 3.54 (GTPγS), and in *F*, 0.44 and 3.56 (Ca^{2+}), and 0.84 and 7.44 (Sr^{2+}).

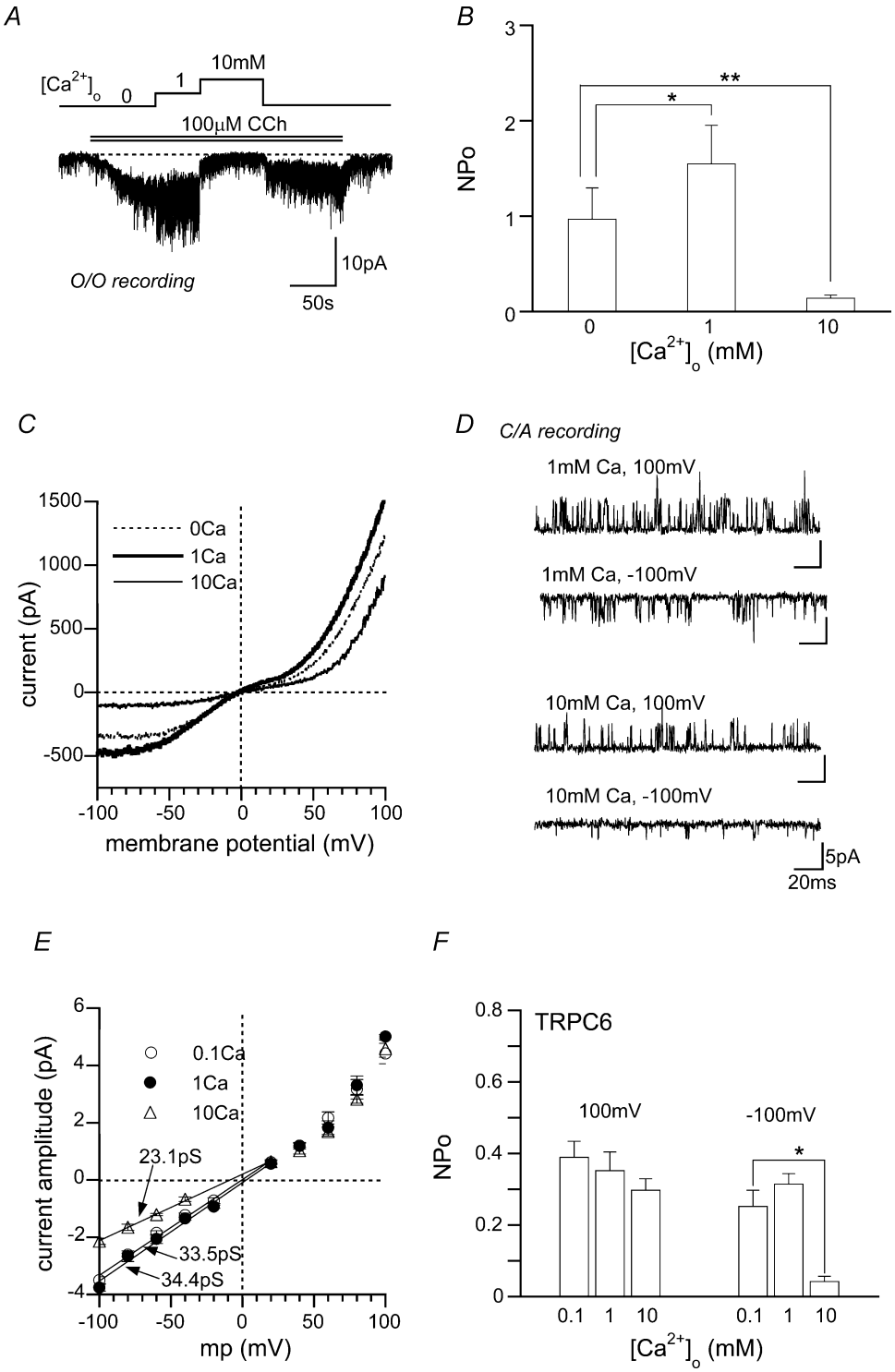

Figure 3. Potentiating and inhibitory effects of Ca_o^{2+} on single TRPC6 channels
A and *B*, O/O recording at −60 mV. O/O membranes were sequentially exposed to CCh (100 μM) and three different $[Ca^{2+}]_o$. A representative record (*A*) and the summary of five separate O/O experiments (*B*). Averaged NP_o is plotted against $[Ca^{2+}]_o$. *C*, typical current–voltage (*I–V*) relationships of I_{TRPC6} at different $[Ca^{2+}]_o$ (0, 1 or 10 mM Ca^{2+} in the bath) evaluated from the same cell. *D–F*, C/A recording. Transmembrane potential was zeroed by high K^+ external solution. Typical examples of single CCh-activated TRPC6 channels at two different Ca^{2+} concentrations in the pipette (i.e. $[Ca^{2+}]_o$ = 1 or 10 mM) and membrane potentials (−100 or 100 mV) (*D*), and *I–V* relationships (*E*) and $[Ca^{2+}]_o$ dependence of NP_o (*F*) of CCh-activated TRPC6 channels. $n = 5$. In *E*, numerals indicate the unitary conductances evaluated by linear data fitting between −100 and 20 mV (continuous lines). $^*P < 0.05$, $^{**}P < 0.01$ with paired *t* test (in *B*) or ANOVA and pooled variance *t* test (in *F*).

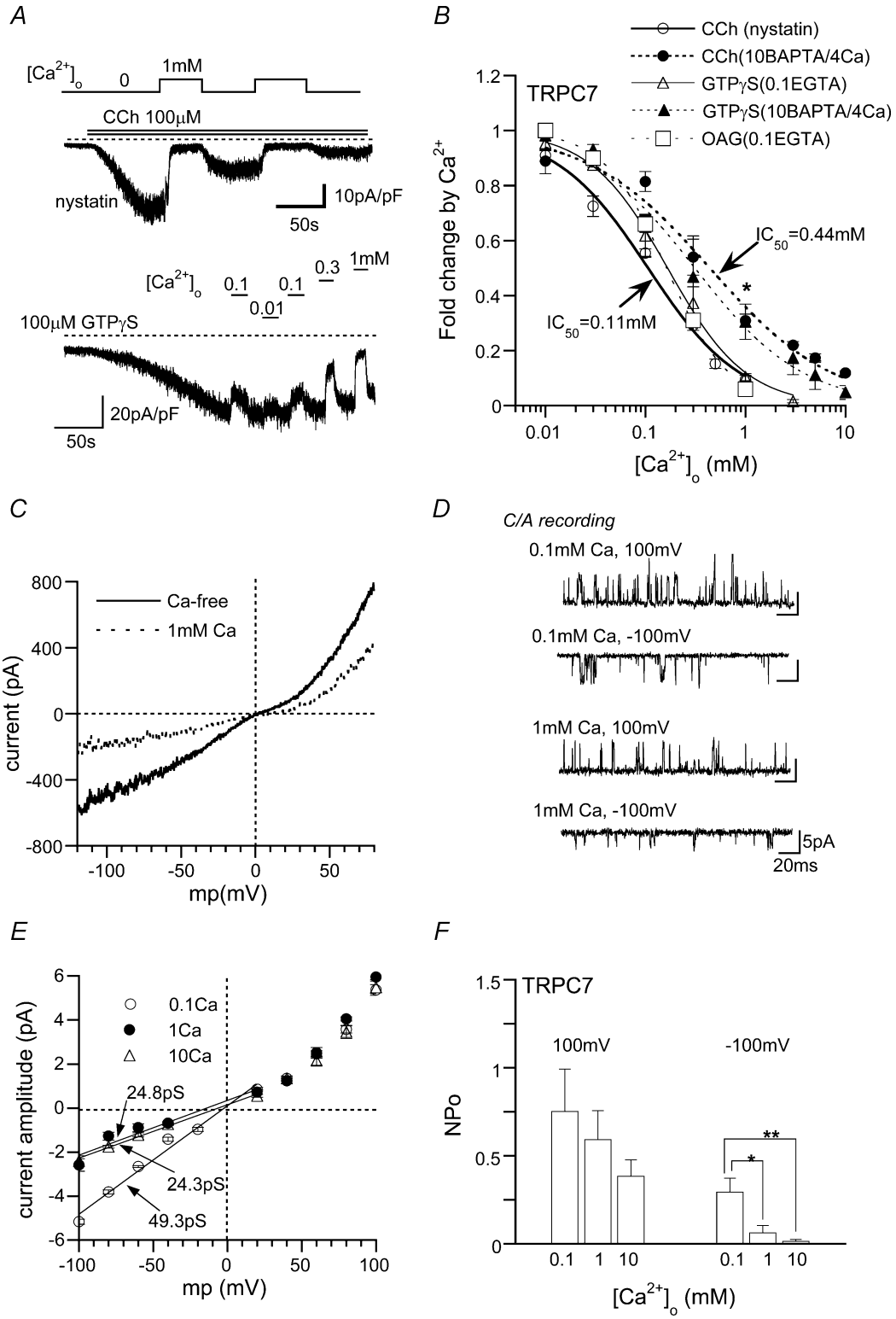

Figure 4. Inhibitory effects of Ca_o^{2+} on I_{TRPC7} and single TRPC7 channels
A, typical examples of Ca_o^{2+}-induced inhibition of I_{TRPC7} recorded at −60 mV, with nystatin-perforated (upper panel) or conventional whole-cell (10 BAPTA/4 Ca internal solution: lower panel) recordings. In the latter, GTPγS (100 μM) was included in a patch pipette. *B*; relationships between $[Ca^{2+}]_o$ and relative I_{TRPC7} amplitude (fold change induced by Ca_o^{2+}) under various conditions. Different activators (100 μM CCh, OAG and GTPγS) and different modes of voltage-clamp (nystatin-perforated and conventional whole-cell recording with either 10 BAPTA/4 Ca or 0.1 EGTA-internal solution) were tested. $^*P < 0.05$ with unpaired *t* test for open *versus* filled circles. Curves

used (i.e. CCh, GTPγS, OAG; Fig. 4*A* and *B*). Part of this inhibition was, however, eliminated by increasing the buffering capacity for $[Ca^{2+}]_i$ (Fig. 4*A versus B*; open *versus* filled circles: * in Fig. 4*B*), suggesting the involvement of elevated $[Ca^{2+}]_i$ in Ca_o^{2+}-induced inhibition.

The fast inhibition of I_{TRPC7} remaining after strong $[Ca^{2+}]_i$ buffering occurred in about a 10-fold lower concentration range of Ca_o^{2+} (apparent IC_{50}: 0.44 mM) as compared with I_{TRPC6}, but showed a very similar voltage dependency to I_{TRPC6}, being characterized by more prominent inhibition of the macroscopic *I–V* relationship and reductions of unitary conductance and NP_o at negative potentials (Fig. 4*C–F*). Furthermore, exchanging the transmembrane (TM) region of TRPC7 with that of TRPC6 converted the fast inhibition caused by 1 mM Ca^{2+} to potentiation (Supplementary Fig. 1). Taken together, these results are consistent with the idea that the site(s) of fast Ca_o^{2+} actions are located on the extracellular side of the TM region, of which only an inhibitory site may commonly exist in TRPC6 and 7 channels.

Mechanisms involved in intracellular Ca^{2+}'s actions on TRPC6 and TRPC7 channels

The abolition of slow potentiating and inactivating effects of Ca_o^{2+} on I_{TRPC6} by vigorous $[Ca^{2+}]_i$ buffering implies that the level of $[Ca^{2+}]_i$ may both positively and negatively regulate TRPC6 channel activity. Consistent with this speculation, when cells were intracellularly perfused with various values of $[Ca^{2+}]_i$, the density of CCh-induced I_{TRPC6} showed a biphasic dependence on $[Ca^{2+}]_i$ consisting of incremental ($< \sim$200 nM) and decremental ($> \sim$200 nM) phases (Fig. 5*A*). A similar $[Ca^{2+}]_i$ dependence was also observed for I_{TRPC7}, but in this case, the range for positive regulation is shifted to much lower concentrations as compared with I_{TRPC6} (Fig. 6*A*). The $[Ca^{2+}]_i$ dependence of TRPC6 and TRPC7 channels did not change appreciably, even when they were activated by OAG (data not shown). It seems thus likely that the site(s) of the actions of intracellular Ca^{2+} (Ca_i^{2+}) are also located on the channel proteins themselves.

Calmodulin (CaM) is a ubiquitous intracellular calcium-binding protein involved in Ca^{2+}-mediated regulation of many ionic channels (Levitan, 1999; Saimi & Kung, 2002). In addition to direct binding to channel proteins, the Ca^{2+}-bound CaM (Ca^{2+}–CaM) activates several physiologically important kinases and phosphatases including CaM-kinase II, myosin light chain kinase (MLCK) and calcineurin, thereby altering the phosphorylated state of channel proteins to modulate their functions (Braun & Schulman, 1995*a*; Rusnak & Mertz, 2000; Kamm & Stull, 2001). To assess the potential importance of these mechanisms in Ca_i^{2+}-mediated regulation of TRPC6 and TRPC7 described above, we next tested how inhibitors for CaM and Ca^{2+}–CaM-dependent enzymes affect these channel functions.

Pretreatment of TRPC6-expressing cells with calmidazolium (CMZ; 3 μM), a potent CaM antagonist (IC_{50}: $\sim$10 nM), or coexpression of a Ca^{2+}-insensitive mutant of CaM (mutCaM), strongly attenuated the activation of I_{TRPC6} by CCh, GTPγS or OAG. (Fig. 5*B* and *C*). Such a marked attenuation also occurred by decreasing $[Ca^{2+}]_i$ to an extremely low level (< 10 nM; Fig. 5*A*), by pretreatment with an organic CaM kinase II inhibitor KN-62 (2 μM), or with intracellular perfusion of CaM-kinase II inhibitory peptide ($CAMK\text{-}IP_{(281–309)}$; Fig. 5*D*). Furthermore, substitution of ATP with its non-hydrolysable analogue AMP-PNP in the patch pipette solution dramatically reduced the I_{TRPC6} density (Fig. 5*D*). These results collectively suggest that phosphorylation by CaM kinase II is a prerequisite for activation of the TRPC6 channel. In contrast, inhibitory peptides for MLCK ($MLCK\text{-}IP_{(11–19)}$, $MLCK\text{-}IP_{(480–501)}$), a non-specific protein phosphatase inhibitor, okadaic acid (10 μM), or a potent calcineurin inhibitor, FK506 (1 μM), did not significantly affect the I_{TRPC6} density (Fig. 5*D*).

In sharp contrast with the critical importance of CaM kinase II for TRPC6 activation, activation of I_{TRPC7} by CCh was not impaired by pretreatment with CMZ (3 μM) or coexpression of mutCaM, but rather enhanced (Fig. 6*B* and *C*; however, spontaneous I_{TRPC7} did not exhibit a significant increase; not shown). Inhibitors for CaM kinase II, MLCK and calcineurin also failed to affect I_{TRPC7} (Fig. 6*E*). These results exclude the requirement of Ca^{2+}–CaM and phosphorylation for TRPC7 channel activation. However, the extent of Ca_o^{2+} (1 mM)-induced inhibition of I_{TRPC7} was significantly reduced by pretreatment with CMZ or coexpression of mutCaM (Fig. 6*D*), being comparable to that observed for strongly $[Ca^{2+}]_i$-buffering conditions (Fig. 4*B*). This observation suggests the presence of some inhibitory actions of Ca^{2+}–CaM on TRPC7 channels. To elucidate these actions more directly, we next employed the inside-out (I/O) configuration of single channel recording.

are drawn according to the results of single Hill fitting (see Methods). $n = 5$–10. *C*, typical *I–V* relationships for I_{TRPC7} obtained just before (Ca^{2+}-free) and after the addition of 1 mM Ca_o^{2+}. *D–F*, C/A recording. Typical examples of single CCh-activated TRPC7 channels at $[Ca^{2+}]_o$ of 0.1, 1 or 10 mM and membrane potentials of −100 or 100 mV (*D*), and *I–V* relationships (*E*) and $[Ca^{2+}]_o$ dependence of NP_o (*F*) of CCh-activated TRPC7 channels. $n = 5$. Continuous lines and the meaning of numerals in *E* are the same as in Fig. 3*E*. $^*P < 0.05$, $^{**}P < 0.01$ with ANOVA and pooled variance *t* test.

Ca^{2+} −CaM actions on TRPC6 and 7 channels

Single TRPC6 or TRPC7 channels recorded in I/O mode with patch pipettes of ordinary size (5–10 MΩ) showed a rapid rundown, which presumably reflects a gradual loss of intracellular constituents maintaining the channel activity (i.e. washout phenomenon). To circumvent this problem, we needed to use patch pipettes having a very low input resistance (1.5–2 MΩ), by which, in more than 30% of patch membranes tested, the decline of channel activity could be minimized over a period of 5–10 min.

Figure 7 demonstrates typical examples of CCh (100 μM)-activated TRPC6 and TRPC7 channel activity at various $[Ca^{2+}]_i$ levels (I/O mode). The activity of the TRPC7 channel was decreased by elevation of $[Ca^{2+}]_i$ in the nanomolar range (< 10–110 nM) and completely suppressed by further increase in $[Ca^{2+}]_i$ (Fig. 7*A* and open circles in *E*). The TRPC6 channel was also subject to inhibition by Ca_i^{2+} but required more than 10-fold higher $[Ca^{2+}]_i$ (1.45 μM) than TRPC7 to be significantly inhibited (Fig. 7*B* and *F*). Ca_i^{2+}-mediated inhibition of TRPC7 channel activity was strongly attenuated by pretreatment with CMZ (3 μM) or coexpression of mutCaM. As demonstrated in Fig. 7*C*, application of CMZ in the C/A configuration gradually enhanced TRPC7 channel activity, which showed, after excision of patch membrane (i.e. I/O mode), a much decreased sensitivity to Ca_i^{2+}; the effective range of $[Ca^{2+}]_i$ to inhibit TRPC7 channels was shifted from nano- to micromolar concentrations (filled circles in Fig. 7*E*). A similar shift was also observed with coexpression of mutCaM (Fig. 7*E*). These results strongly suggest that TRPC7 channel activity is negatively regulated by Ca^{2+}−CaM.

The effects of CMZ and mutCaM on single TRPC6 channels were entirely different from those on TRPC7 channels. Consistent with their effects observed for macroscopic I_{TRPC6}, application of CMZ greatly diminished the CCh-induced TRPC6 channel activity in C/A mode, and subsequent exposure of excised membrane to various $[Ca^{2+}]_i$ levels (I/O mode) could not restore the channel activity (Fig. 7*D* and *F*). Coexpression of mutCaM produced essentially the same results (Fig. 7*F*). These

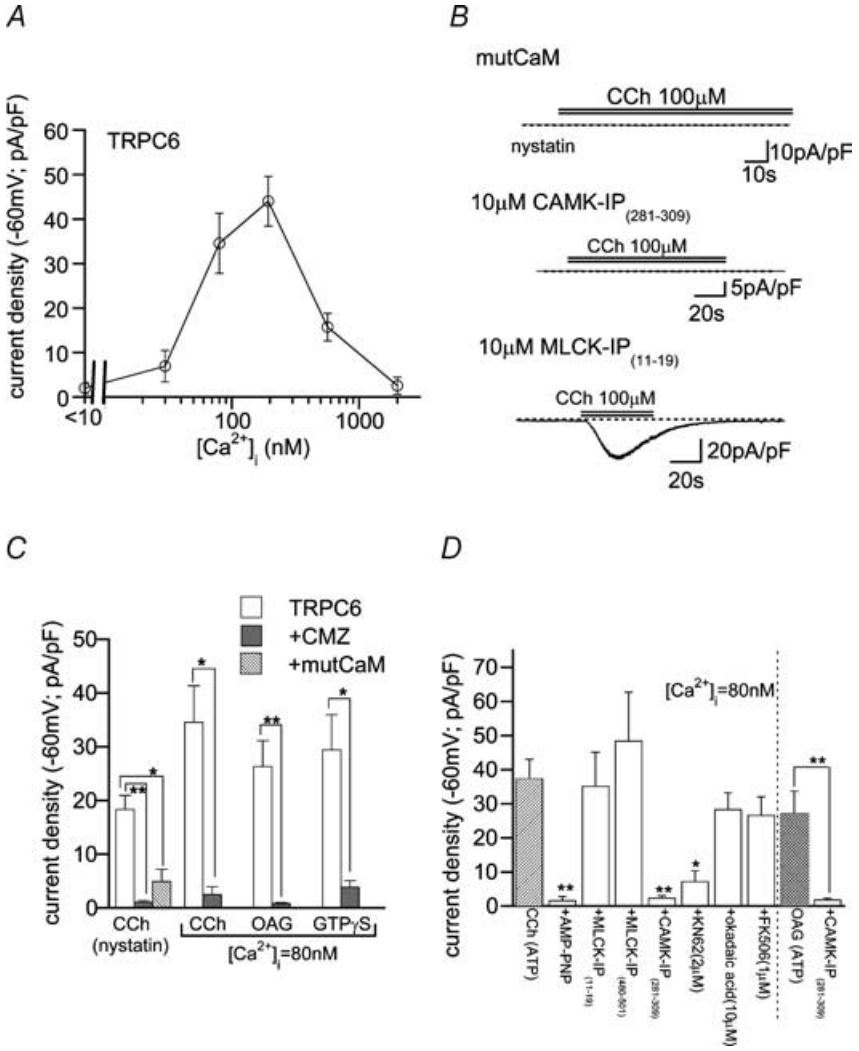

Figure 5. Essential requirement of CaM-kinase II-mediated phosphorylation for TRPC6 channel activation
Bath: 1 mM Ca^{2+}-containing external solution. *A*, relationship between $[Ca^{2+}]_i$ and CCh (100 μM)-evoked I_{TRPC6} density. $n = 5$–19. *B*, typical examples of I_{TRPC6} recorded from cells coexpressing Ca^{2+}-insensitive mutant calmodulin (mutCaM; nystatin-perforated recording; top trace) and those intracellularly perfused (> 5min; whole-cell; $[Ca^{2+}]_i$: 80 nM; 10 mM BAPTA/4 mM Ca^{2+}) with 10 μM CaM-kinase inhibitory peptide (middle trace) or MLCK inhibitory peptide (bottom trace). *C*; effects of calmidazolium (CMZ; 3 μM) pretreatment or mutCaM coexpression on I_{TRPC6} evoked by 100 μM CCh, OAG or GTPγS. $n = 5$–15. *D*; effects of kinase and phosphatase inhibitors on I_{TRPC6} evoked by 100 μM CCh or OAG. Whole-cell recording ($[Ca^{2+}]_i$: 80 nM). $n = 7$–17. $^*P < 0.05$, $^{**}P < 0.01$ with unpaired *t* test (*C*: rightmost two columns in *D*) and with ANOVA and pooled variance *t* test (the other columns in *D*: control is hatched).

results confirm that the Ca^{2+}−CaM-mediated process is obligatory for TRPC6 channel activation. However, we cannot exclude the possibility that inhibition by Ca^{2+}−CaM observed at micromolar $[Ca^{2+}]_i$, which was not experimentally seen after abolition of the activation process, may also exert some modulatory role on TRPC6 channels.

The mechanism for the negative regulation of TRPC7 channels by Ca^{2+}−CaM seems compatible with a recently proposed hypothesis of competitive regulation by CaM and IP_3 of TRPC3 for its common binding domain (e.g. CIRB; see Introduction). Addition of IP_3 (10 μM) increased single TRPC7 activity, and this was significantly counteracted by elevated $[Ca^{2+}]_i$ or exogenously applied CaM (1 μM) (Fig. 8*A* and *B*). Macroscopic I_{TRPC7} evoked by CCh or OAG was also greatly enhanced by intracellular perfusion of IP_3 (Fig. 8*D*; there was, however, no dramatic increase in spontaneous I_{TRPC7}; 5.5 ± 1.4 *versus* 7.4 ± 1.3 pA pF^{-1} without and with 10 μM IP_3, respectively; $n = 7$). In contrast, IP_3 exerted little effect on TRPC6 at either the whole-cell or the single channel level (Fig. 8*B* and *D*). Instead, as reported recently (Estacion *et al.* 2004), marked enhancement of OAG-induced I_{TRPC6} occurred by pretreatment with a subthreshold activating concentration of CCh (0.5 μM; Fig. 8*C* and *D*). At least under our experimental conditions, the major part of this enhancement seems ascribable to synergistic effects of Ca_i^{2+}, as it was observed only with weak $[Ca^{2+}]_i$ buffering; OAG (100 μM)-induced I_{TRPC6} recorded with 10 BAPTA/4 Ca internal solution was not significantly affected by pretreatment with 0.5 μM CCh (at −60 mV; 27.0 ± 6.7 pA pF^{-1} ($n = 5$) *versus* 26.3 ± 4.8 pA pF^{-1} ($n = 6$) for control and 0.5 μM CCh pretreatment, respectively).

Differential regulation by Ca^{2+}−CaM and IP_3 observed between TRPC7 and 6 channels probably reflects their C-terminal differences. Their chimeras with exchanged C-termini T667 and T776 showed essentially the same dependence on Ca^{2+}−CaM and IP_3 as TRPC7 and TRPC6, respectively (Supplementary Fig. 2).

Involvement of PKC in TRPC6 inactivation

According to previous studies (Trebak *et al.* 2003; Estacion *et al.* 2004), protein kinase C (PKC) negatively regulates some TRPC members including TRPC6. This raises the possibility that activation of PKC may be involved in the rapid inactivation process of I_{TRPC6} in the presence

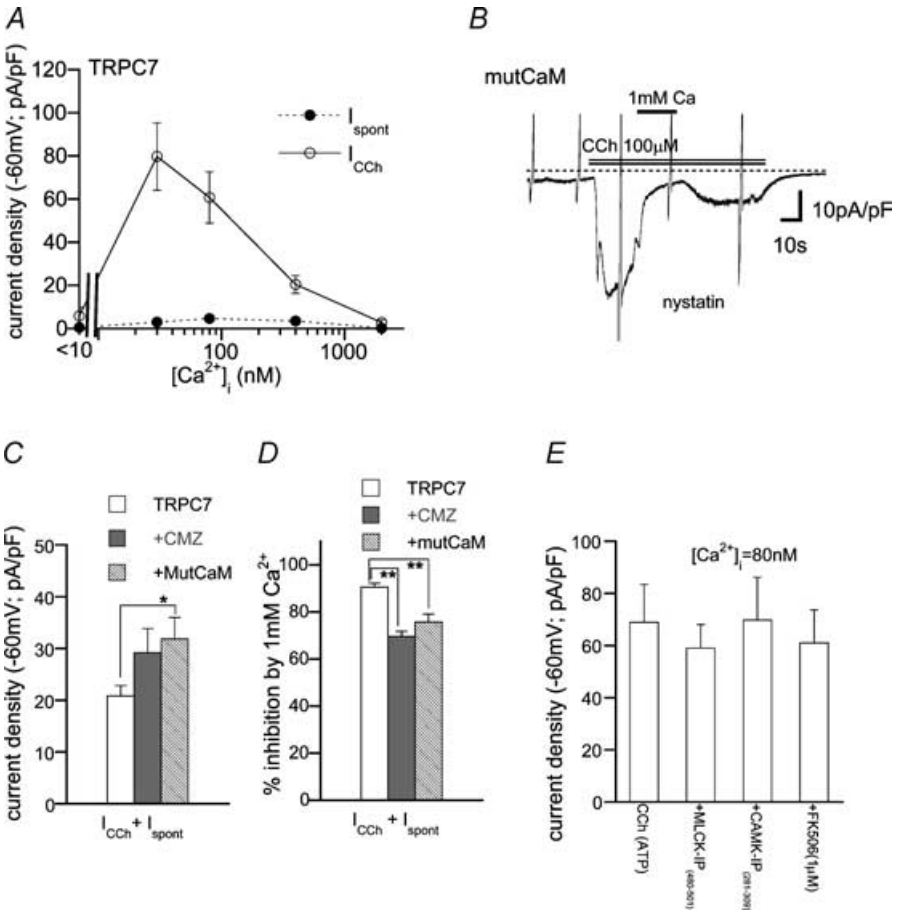

Figure 6. CaM-mediated inhibition of I_{TRPC7}
Bath: Ca^{2+}-free external solution. *A*, relationship between $[Ca^{2+}]_i$ and spontaneously activated (I_{spont}) or CCh (100 μM)-evoked (I_{CCh}) I_{TRPC7}. $n = 8$–14. Whole-cell recording. *B*, a typical example of I_{TRPC7} recorded from a mutCaM-coexpressing cell under nystatin-perforated voltage clamp. *C* and *D*, CMZ pretreatment (3 μM) or mutCaM coexpression enhances the density (*C*) and relieves Ca_o^{2+} (1 mM)-induced inhibition (*D*) of I_{TRPC7}. Nystatin-perforated recording. $n = 7$–20. *E*, ineffectiveness of inhibitors for MLCK, CaMKII and calcineurin for I_{TRPC7}. $n = 5$–8. $^*P < 0.05$, $^{**}P < 0.01$ with ANOVA and pooled variance *t* test.

of Ca_o^{2+} (Fig. 1*A* and *B*) and its decreased current density at micromolar $[Ca^{2+}]_i$ (Fig. 5). Consistent with this expectation, inclusion of a PKC inhibitor, calphostin C (500 nM) or a PKC inhibitory peptide (PKC-$IP_{(19–36)}$: 5 μM) in the patch pipette significantly decelerated the time course of inactivation (or decreased $\tau_{10–90}$ value; Fig. 9*A* and *B*) and enhanced the I_{TRPC6} density at micromolar $[Ca^{2+}]_i$ (Fig. 9*C*). Conversely, activation of

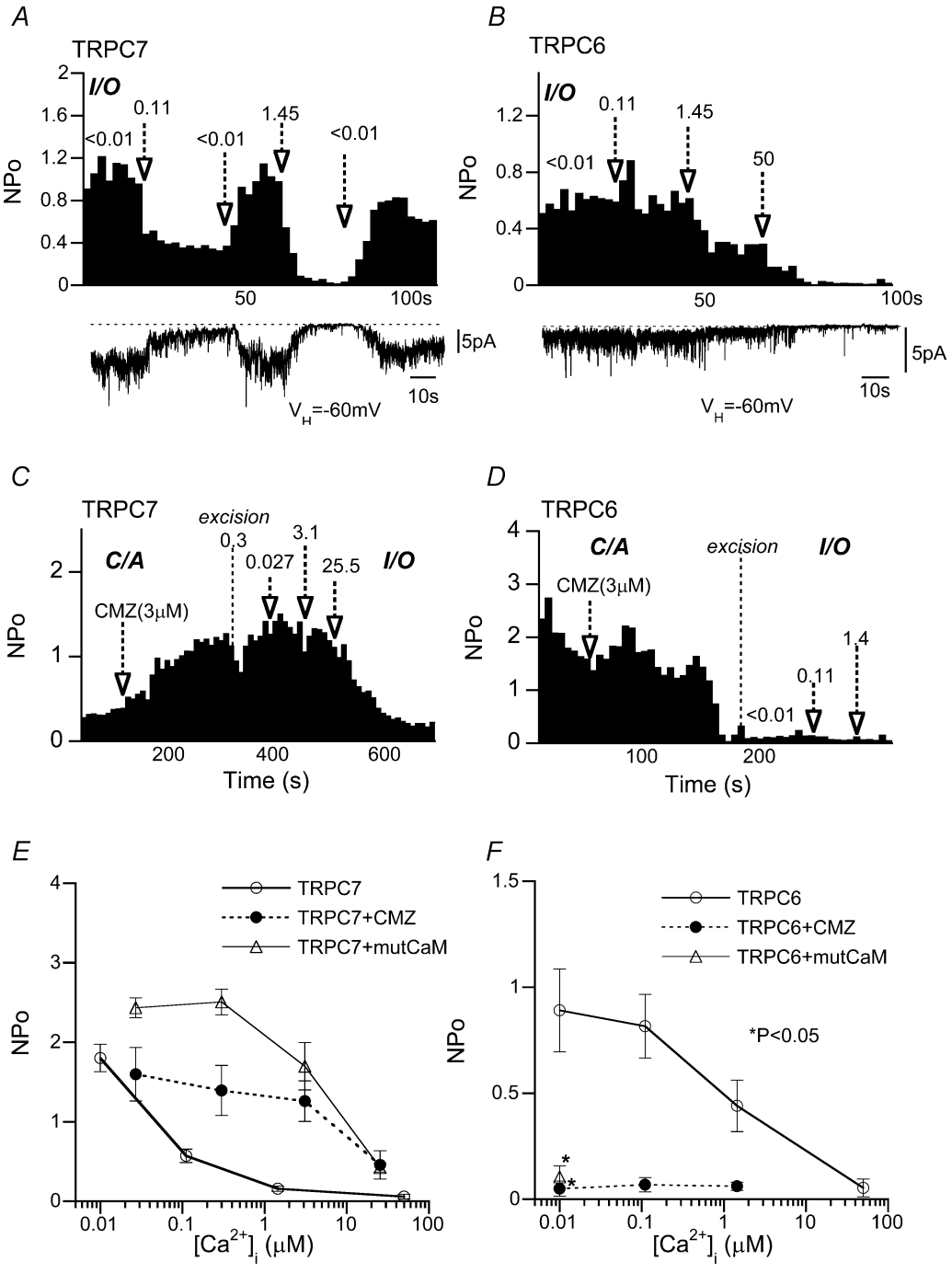

Figure 7. Differential dependence of single TRPC6 and TRPC7 channels on Ca_i^{2+} and CaM
I/O recording at −60 mV. *A* and *B*, typical traces (lower panels) and corresponding NP_o *versus* time plots (upper panels) for CCh-activated TRPC7 (*A*) and TRPC6 (*B*) channels at different $[Ca^{2+}]_i$. Numerals and arrows indicate the value of $[Ca^{2+}]_i$ (micromolar) and the timing of solution change, respectively. *C* and *D*, effects of CMZ on CCh-activated TRPC7 (*C*) and TRPC6 (*D*) channels. NP_o *versus* time plots. CMZ (3 μM) was applied in C/A mode, and then patch membranes were excised (I/O mode). *E* and *F*, NP_o–$[Ca^{2+}]_i$ relationships (I/O mode) for CCh-activated TRPC7 and TRPC6 channels, without (open circles) or with CMZ (3 mM) treatment (filled circles) or mutCaM coexpression (open triangles). $n = 5–9$. $^*P < 0.05$ with pooled variance *t* test for filled circle or open triangle *versus* open circle at the same $[Ca^{2+}]_i$ (control).

PKC by a phorbol ester, PDBu (1 μM; pretreated 10 min), caused almost complete suppression of I_{TRPC6} (Fig. 9*C*). Similar enhancement of current density by PKC inhibitors and inhibition by PDBu were also observed for I_{TRPC7} (Fig. 9*C*).

Discussion

TRPC6 and 7 share more than 70% identity in the overall amino acid sequence (N-terminus: 80%; transmembrane region: 77%; C-terminus: 73%) and both code for Ca^{2+}-permeable cation channels activated by diacylglycerol (Hofmann *et al.* 1999; Okada *et al.* 1999). Despite these molecular and functional similarities, the results of the present study have provided the evidence that heterologously expressed TRPC6 and 7 channels undergo contrasting regulation by Ca^{2+} from both extracellular and intracellular sides, via CaM-dependent and - independent mechanisms.

Whole-cell (with 10 mM BAPTA) and single channel data (Fig. 4) together suggest that the major part of fast voltage-dependent inhibitory actions by Ca_o^{2+} on I_{TRPC7} is ascribable to its interaction with an 'extracellular' site(s) which can sense the transmembrane potential. A similar inhibitory site having a weaker efficacy is probably present in TRPC6 channels (Figs 2 and 3). In

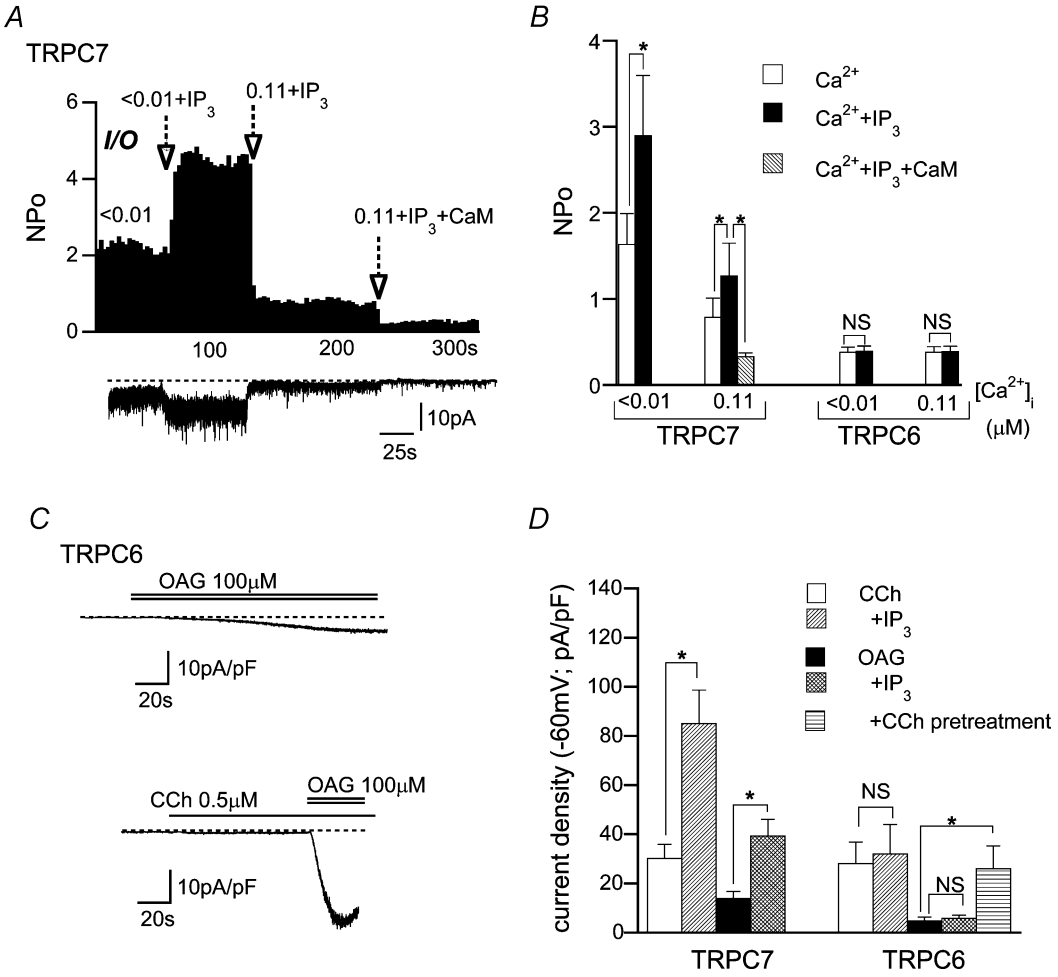

Figure 8. Intracellular IP_3 differentially affects single TRPC7 and TRPC6 channel activity
A, typical trace (lower panel) and corresponding NP_o *versus* time plot (upper panel) for CCh-activated TRPC7 channel activity at two different $[Ca^{2+}]_i$ values (< 10 nM and 0.11 μM) with IP_3 (10 μM) or wild-type CaM (1 μM). I/O recording at −60 mV. *B*, summary of the effects of Ca_i^{2+}, IP_3 (10 μM) or CaM (1 μM) on single TRPC7 and TRPC6 channel activity evaluated from experiments such as shown in *A*. $n = 5$–8. *C*, typical examples of OAG (100 μM)-induced I_{TRPC6} at −60 mV with (lower panel) or without (upper panel) a subthreshold activating concentration of CCh (0.5 μM). *D*, summary of the effects of intracellular IP_3 (10 μM; added in the pipette) or a subthreshold concentration of CCh (0.5 μM) on I_{TRPC6} and I_{TRPC7}. $n = 5$–7. In *C* and *D*, bath and pipette contained 1 mM Ca^{2+}-containing external and 0.1 EGTA internal solutions, respectively. $^*P < 0.05$ with unpaired *t* test or ANOVA and pooled variance *t* test.

contrast, the fast potentiating effect of Ca_o^{2+} is unique to TRPC6, did not show voltage dependence and was not associated with changes in unitary conductance (compare 0.1 and 1 mM in Fig. 3*E*), but also probably occurred through the extracellular actions of Ca^{2+}, as unequivocally demonstrated by the O/O recording (Fig. 2*A* and *B*). The finding that the type of TM region critically determines the pattern of response to Ca_o^{2+} (i.e. 'inhibitory' or 'facilitatory'; Supplementary Fig. 1) further reinforces this speculation. These extracellular Ca^{2+} effects may most simplistically be accounted for by the permeation blockade and/or stabilization of gating in 'non-conductive' states by Ca_o^{2+}, which are often found in many cation-selective channels (e.g. Hille, 2001).

Complex extracellular actions of Ca^{2+} and of its mimetic lanthanides (La^{3+} and Gd^{3+}), which are strongly reminiscent of Ca_o^{2+} actions on TRPC6 and 7, have recently been reported for heterologously expressed mouse TRPC5 channel (Jung *et al.* 2003). In this channel, the effect of lanthanides is biphasic with concentration-dependent potentiation in the low micromolar range and inhibition in a higher concentration range, whereas that of Ca^{2+} is merely facilitatory only at high millimolar concentrations. Site-directed mutagenesis has revealed that three glutamate residues adjacent to the putative pore-forming loop (Glu^{543}, Glu^{595}, Glu^{598}) are crucial for the observed La^{3+}- as well as Ca^{2+}-induced potentiation (Jung *et al.* 2003). However, alignments of the TM5–TM6 linker region of TRPC5, 6 and 7 (Supplementary Fig. 3) indicate little similarity present for these glutamates between the three TRPC channels (see also Jung *et al.* 2003). Except for Glu^{598}, negatively charged residues corresponding to Glu^{543} or Glu^{595} are absent in TRPC6 and 7, which instead possess four additional glutamates or aspartate in the more central part. Furthermore, the overall amino acid sequence of TRPC6 and 7 in this linker region, especially the number and position of negatively charged residues, is highly homologous (Supplementary Fig. 3), thus suggesting that these residues might not suffice to elucidate the differential effects of Ca_o^{2+} on TRPC6 and 7 channels.

The observed $[Ca^{2+}]_o$ sensitivity of recombinant TRPC6 channel is substantially different from that reported for a number of native ROC channels in which this protein is probably involved (Inoue *et al.* 2001; Jung *et al.* 2002). For instance, the α1-adrenonceptor-activated cationic channel (α1-AD-NSCC) in portal vein smooth muscle displays much higher sensitivity to Ca_o^{2+} potentiation ($EC_{50} = 3\ \mu M$) showing a rapid declining feature (Helliwell & Large, 1998), and is also potentiated by submillimolar concentrations of Ba^{2+} and Sr^{2+} (Aromolaran & Large, 1999). However, in the present

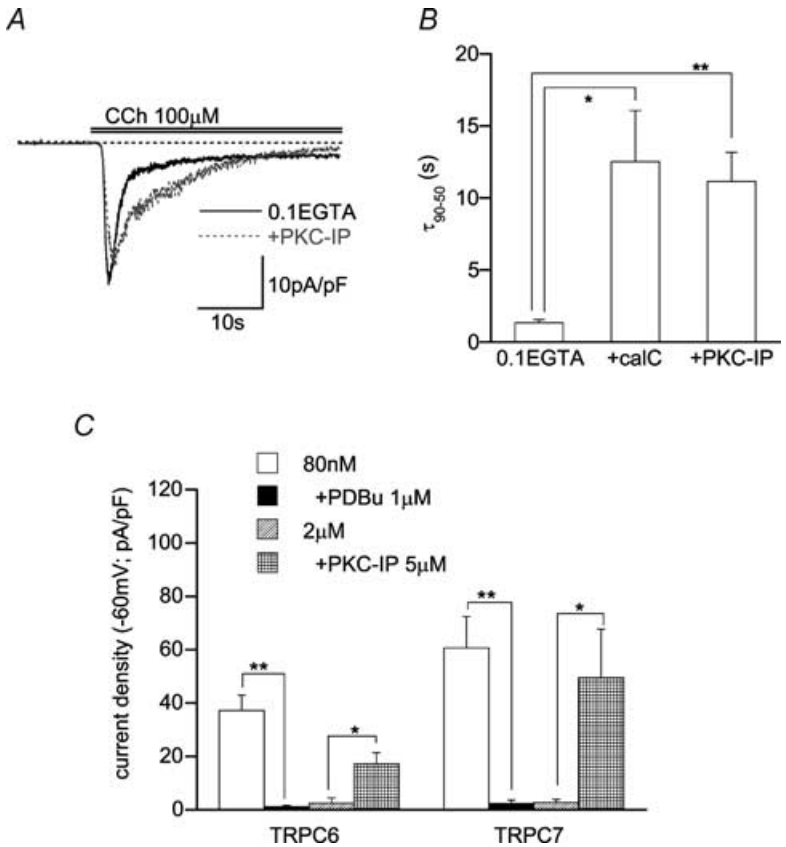

Figure 9. PKC mediates inactivation of TRPC6 and TRPC7 channels
A, representative records of CCh-evoked I_{TRPC6} with or without PKC inhibitory peptide ($PKC\text{-}IP_{(19–36)}$, 5 μM) in the pipette. *B*, effects of PKC inhibitors on the inactivation time of I_{TRPC6} ($\tau_{90–50}$; see Fig. 1 legend); control (0.1 EGTA internal solution): pretreatment with calphostin C (500 nM, 5min, middle): intracellular perfusion of $PKC\text{-}IP_{(19–36)}$ (5 μM, 5min, right). $n = 7–12$. Recording conditions in *A* and *B* were the same as in Fig. 8*C* and *D*. *C*, effects of PKC inhibitors and activators on I_{TRPC6} or I_{TRPC7} density at two different $[Ca^{2+}]_i$ levels. $n = 5–12$. $^*P < 0.05$, $^{**}P < 0.01$ with unpaired *t* test (in *C*) or ANOVA and pooled variance *t* test (in *B*).

study, Ba^{2+} was found to be ineffective in causing either potentiation or inhibition of expressed TRPC6 channels, and their potentiation by Ca^{2+} and Sr^{2+} was rather long-lasting (Figs 1*D* and 2*D*). A more strikingly different $[Ca^{2+}]_o$ sensitivity is found for TRPC6-like currents in A7r5 cells, where millimolar Ca_o^{2+} exerts only inhibitory actions, although reduction of this current by changing $[Ca^{2+}]_o$ from 200 μM to nominally zero suggests a stimulatory role of Ca_o^{2+} (Ba^{2+} and Sr^{2+} are, however, ineffective; Jung *et al.* 2002). A possible molecular background for such discrepancies is that these native TRPC6-like channels may be heteromultimerically assembled with other endogenously expressed TRP isoforms, thereby acquiring diverse divalent cation sensitivities. In support of this possibility, TRPC6 has been shown to coimmunoprecipitate with TRPC3 and 7 in adult tissues (Hofmann *et al.* 2002; Goel *et al.* 2002) and in embryonic brain interact with other TRPC isoforms in complex combinations (Strübing *et al.* 2003), and the presence of some of these isoforms has been confirmed by RT-PCR technique in portal vein myocytes and A7r5 cells (Inoue *et al.* 2001; Jung *et al.* 2002). However, it should be noted that the expression system used in this study (HEK293 cells) has been reported to endogenously express several TRPC isoforms including TRPC1, 3, 4 and 6 (Garcia & Schilling, 1997). Considering this fact, we cannot completely exclude the possibility that overexpressed TRPC6 or 7 channels could also be affected by these endogenously TRPC proteins thus bearing somewhat altered properties as compared with genuine homomeric channels.

Single channel data in large I/O membranes have indicated that, once receptor-activated, TRPC7 channels are concentration-dependently inhibited by Ca_i^{2+} in the nanomolar range. These effects are probably mediated via CaM-dependent actions on its C-terminus, as indicated by mutCaM coexpression and TRPC6/7 chimera experiments. Previous biochemical studies have shown that all TRPC members possess a common binding region for CaM and IP_3 receptor (IP_3R) on the C-terminus (CIRB domain), to which CaM binds in a strictly Ca^{2+}-dependent manner (Tang *et al.* 2001). It has been hypothesized that under resting conditions, CaM bound to this region tonically inhibits TRPC3 channels, and its displacement by activated IP_3R (by receptor stimulation) or its inactivation by the CaM antagonist CMZ leads to channel activation (Zhang *et al.* 2001). Overall, this picture seems to apply to TRPC7; pretreatment with CMZ or coexpression of mutCaM enhanced CCh-activated TRPC7 channel activity at both single channel (C/A mode; Fig. 7) and whole-cell (Fig. 6) levels; in I/O recording, inhibitory effects of Ca_i^{2+} on the TRPC7 channel, which were strongly attenuated by CMZ or mutCaM (Fig. 7), were antagonized and enhanced by IP_3 and CaM, respectively (Fig. 8). However, the observed $[Ca^{2+}]_i$ range for CaM-dependent TRPC7 channel inhibition (apparent $IC_{50} \approx 100$ nM; Fig. 7) is far lower when compared to the Ca^{2+}-dependence of CaM binding domain (i.e. CIRB) evaluated *in vitro* (Tang *et al.* 2001). The effect of Ca_i^{2+} still persisted even after exposure to a very low $[Ca^{2+}]_i$ level (< 10 nM) which was expected to unbind CaM (Fig. 7*A*). Coexpression of mutCaM enhanced the magnitude of I_{TRPC7}, but did not appreciably induce a current by itself unless the receptor was stimulated (e.g. Fig. 6*B*). All these findings are not simply compatible with the antagonism between CaM and IP_3R for channel activation (Zhang *et al.* 2001). The most straightforward interpretation of the above results is that CaM is constitutively bound to TRPC7 channel C-terminus and negatively regulates the channel activity in a Ca^{2+}-dependent fashion regardless of receptor activation process. Thus, the role of CaM would not be obligatory for TRPC7 channel activation but rather modulatory as a negative feedback operating during receptor stimulation. However, despite the observed $[Ca^{2+}]_i$ range for negative regulation of single TRPC7 channels (Fig. 7*E*) roughly matching that for I_{TRPC7} (Fig. 6*A*), at an extremely low $[Ca^{2+}]_i$ (< 10 nM), receptor activation of I_{TRPC7} was severely impaired. This is unexpected from single channel recordings, and unlikely to involve the actions of CaM, IP_3R or phosphorylation, e.g. by CAMKII (see above). It seems thus likely that an additional, as-yet-unidentified, Ca^{2+}-dependent mechanism participates in the activation process of TRPC7 channels.

Despite the presence of almost identical CaM binding domain (CIRB; Tang *et al.* 2001), the inhibitory effect of Ca_i^{2+} on single TRPC6 channels is much weaker than TRPC7 (it occurred only at micromolar $[Ca^{2+}]_i$), and intracellular application of IP_3 failed to activate or enhance the channel activity at whole-cell and single channel levels (Fig. 8). This excludes the involvement of competitive regulation by Ca^{2+}–CaM and IP_3R in the TRPC6 channel activation process. Instead, we have found that activation of macroscopic TRPC6 current is positively regulated by nanomolar Ca_i^{2+} and highly susceptible to procedures that eliminate intracellular ATP and CaM or directly inhibit CAMKII, regardless of the activator (i.e. CCh or OAG) (Figs 5 and 7). These results are consistent with the idea that phosphorylation by CaMKII is an obligatory step for TRPC6 channel activation and occurs independently of the process of generating DAG. Similar CaMKII phosphorylation-mediated activation has also been reported for epithelial Ca^{2+}-activated non-selective cation channels, the properties of which are strongly reminiscent of some TRP members (Braun & Schulman, 1995*b*).

Somewhat puzzlingly, however, activation of the native counterpart of TRPC6, α1-AD-NSCC in vascular smooth muscle, has been reported to be mediated by MLCK rather than CAMKII (Aromolaran *et al.* 2000). In this native channel, MLCK-specific peptides,

one of which ($MLCK_{(11–19)}$ amide) was found to be ineffective for expressed TRPC6 channel in this study, strongly prevented the activation of α1-AD-NSCC. One plausible explanation for this discrepancy is that a rather muscle-specific distribution of MLCK may allow its preferential interaction with the TRPC6 channel in muscle tissues (Kamm & Stull, 2001) whereas in other tissues, the more ubiquitous CaMKII may play a similar role. However, it should be pointed out that while CaMKII can target a multitude of substrates including ion channels (Braun & Schulman, 1995*a*), the only known physiological target of MLCK is myosin, which is implicated in the regulation of muscle contraction and cytoskeletal activity but not directly in channel activation (Kamm & Stull, 2001). These discrepancies, together with the fact that synergism between IP_3 and OAG observed for α1-AD-NSCC activation (Albert & Large, 2003) is deficient in expressed TRPC6 channels (Fig. 8; Estacion *et al.* 2004), again suggest that essential differences may be present in subunit compositions or accessory regulatory mechanisms between these two channels. Obviously, more studies will be needed to elucidate the exact mechanism underlying phosphorylation-mediated activation of the TRPC6 channel.

In summary, the activity of the TRPC6 channel is probably regulated by Ca^{2+} in a multifold fashion. In physiological ionic milieu, in addition to direct tonic enhancement by Ca^{2+}_o, Ca^{2+}_i-dependent mechanisms seem to dynamically regulate TRPC6 channels during PLC-linked receptor stimulation. In the early phase, Ca^{2+} released from internal stores via activated IP_3R and Ca^{2+} influx through activated TRPC6 channels by DAG generation elevate $[Ca^{2+}]_i$ thereby facilitating the channel activation process via CaMKII-mediated phosphorylation (Fig. 5). When the elevation of $[Ca^{2+}]_i$ is sustained, however, this turns to inactivation via PKC activation (Fig. 9). Such sequential activation of kinases can be seen as accelerated activation and inactivation processes by Ca^{2+}_o (Fig. 1*A* and *C*). In contrast, Ca^{2+} regulates TRPC7 channels almost negatively via direct extracellular, and Ca^{2+}–CaM- (but phosphorylation-independent) and PKC-dependent mechanisms (Figs 4, 7 and 9). In this channel, generation of IP_3 seems to synergistically enhance the channel activity with its primary activator DAG (Fig. 8).

Multifold regulation by Ca^{2+} reminiscent of TRPC6 has been reported for some native ROC channels. For instance, muscarinic cation channels in gastrointestinal smooth muscle has been shown to be strongly potentiated by $[Ca^{2+}]_i$ elevation (Inoue & Isenberg, 1990; Pacaud & Bolton, 1991), part of which may involve a Ca^{2+}–CaM–MLCK-dependent pathway (Kim *et al.* 1995; Kim *et al.* 1997). This mechanism seems to operate as an effective positive feedback synchronized with action potentials and IP_3-mediated intracellular Ca^{2+} release, contributing to enhanced excitatory actions of visceral cholinergic nerves on gut motility (Kuriyama *et al.* 1998). In contrast, prolonged $[Ca^{2+}]_i$ elevation inactivates these channels and terminates the muscarinic response rapidly (Kim *et al.* 1998; Zholos *et al.* 2003). A similar situation may hold for the α1-AD-NSCC in portal vein smooth muscle, in which the molecular contribution of TRPC6 has been more unequivocally demonstrated (Inoue *et al.* 2001; Large, 2002). In this respect, the results of this study would provide an important molecular basis for elucidating such multifold effects of Ca^{2+} in native tissues.

References

Albert AP & Large WA (2003). Synergism between inositol phosphates and diacylglycerol on native TRPC6-like channels in rabbit portal vein myocytes. *J Physiol* **552**, 789–795.

Aromolaran AS, Albert AP & Large WA (2000). Evidence for myosin light chain kinase mediating noradrenaline-evoked cation current in rabbit portal vein myocytes. *J Physiol* **524**, 853–863.

Aromolaran AS & Large WA (1999). Comparison of the effects of divalent cations on the noradrenaline-evoked cation current in rabbit portal vein smooth muscle cells. *J Physiol* **520**, 771–782.

Boulay G (2002). Ca^{2+}-calmodulin regulates receptor-operated Ca^{2+} entry activity of TRPC6 in HEK-293 cells. *Cell Calcium* **32**, 201–207.

Boulay G, Brown DM, Qin N, Jiang M, Dietrich A, Zhu MX, Chen Z, Birnbaumer M, Mikoshiba K & Birnbaumer L (1999). Modulation of Ca^{2+} entry by polypeptides of the inositol 1,4,5-trisphosphate receptor (IP3R) that bind transient receptor potential (TRP): evidence for roles of TRP and IP3R in store depletion-activated Ca^{2+} entry. *Proc Natl Acad Sci U S A* **96**, 14955–14960.

Braun AP & Schulman H (1995*a*). The multifunctional calcium/calmodulin-dependent protein kinase: from form to function. *Annu Rev Physiol* **57**, 417–445.

Braun AP & Schulman H (1995*b*). A non-selective cation current activated via the multifunctional Ca^{2+}-calmodulin-dependent protein kinase in human epithelial cells. *J Physiol* **488**, 37–55.

Brooks SP & Storey KB (1992). Bound and determined: a computer program for making buffers of defined ion concentrations. *Anal Biochem* **14**, 119–126.

Clapham DE, Runnels LW & Strübing C (2001). The TRP ion channel family. *Nat Rev Neurosci* **2**, 387–396.

Estacion M, Li S, Sinkins WG, Gosling M, Bahra P, Poll C, Westwick J & Schilling WP (2004). Activation of human TRPC6 channels by receptor stimulation. *J Biol Chem* **279**, 22047–22056.

Garcia RL & Schilling WP (1997). Differential expression of mammalian TRP homologues across tissues and cell lines. *Biochem Biophys Res Commun* **239**, 279–283.

Goel M, Sinkins WG & Schilling WP (2002). Selective association of TRPC channel subunits in rat brain synaptosomes. *J Biol Chem* **277**, 48303–48310.

Hardie RC (1995). Photolysis of caged Ca^{2+} facilitates and inactivates but does not directly excite light-sensitive channels in *Drosophila* photoreceptors. *J Neurosci* **15**, 889–902.

Helliwell RM & Large WA (1998). Facilitatory effect of Ca^{2+} on the noradrenaline-evoked cation current in rabbit portal vein smooth muscle cells. *J Physiol* **512**, 731–741.

Hille B (2001). *Ion Channels of Excitable Membranes*, 3rd edn. Sunauer Associates, Inc., Sunderland, MA, USA.

Hoffmann T, Obukhov AG, Schaefer M, Harteneck C, Gudermann T & Schultz G (1999). Direct activation of human TRPC6 and TRPC3 channels by diacylglycerol. *Nature* **397**, 259–263.

Hofmann T, Schaefer M, Schultz G & Gudermann T (2002). Subunit composition of mammalian transient receptor potential channels in living cells. *Proc Natl Acad Sci U S A* **99**, 7461–7466.

Horn R & Marty A (1988). Muscarinic activation of ionic currents measured by a new whole-cell recording method. *J General Physiol* **92**, 145–159.

Inoue R (1991). Effect of external Cd^{2+} and other divalent cations on carbachol-activated non-selective cation channels in guinea-pig ileum. *J Physiol* **442**, 447–463.

Inoue R & Isenberg G (1990). Intracellular calcium ions modulate acetylcholine-induced inward current in guinea-pig ileum. *J Physiol* **424**, 73–92.

Inoue R & Ito Y (2000). Intracellular ATP slows time-dependent decline of muscarinic cation current in guinea pig ileal smooth muscle. *Am J Physiol Cell Physiol* **279**, C1307–C1318.

Inoue R, Morita H & Ito Y (2004). Newly emerging Ca^{2+} entry channel molecules that regulate the vascular tone. *Expert Opin Ther Targets* **8**, 321–334.

Inoue R, Okada T, Onoue H, Hara Y, Shimizu S, Naitoh S, Ito Y & Mori Y (2001). The transient receptor potential protein homologue TRP6 is the essential component of vascular α_1-adrenocepotor-activated Ca^{2+}-permeable cation channel. *Circ Res* **88**, 325–332.

Jung S, Mühle A, Schaefer M, Strotmann R, Schultz G & Plant TD (2003). Lanthanides potentiate TRPC5 currents by an action at extracellular sites close to the pore mouth. *J Biol Chem* **278**, 3562–3571.

Jung S, Strotmann R, Schultz G & Plant TD (2002). TRPC6 is a candidate channel involved in receptor-stimulated cation currents in A7r5 smooth muscle cells.*Am J Physiol Cell Physiol* **282**, C347–C359.

Kamm KE & Stull JT (2001). Dedicated myosin light chain kinases with diverse cellular functions. *J Biol Chem* **276**, 4527–4530.

Kamouchi M, Philipp S, Flockerzi V, Wissenbach U, Mamin A, Raeymaekers L, Eggermont J, Droogmans G & Nilius B (1999). Properties of heterologously expressed hTRP3 channels in bovine pulmonary artery endothelial cells. *J Physiol* **518**, 345–358.

Kim SJ, Ahn SC, So I & Kim KW (1995). Role of calmodulin in the activation of carbachol-activated cationic current in guinea-pig gastric antral myocytes. *Pflugers Arch* **430**, 757–762.

Kim YC, Kim SJ, Kang TM, Suh SH, So I & Kim KW (1997). Effects of myosin light chain kinase inhibitors on carbachol-activated nonselective cationic current in guinea-pig gastric myocytes. *Pflugers Arch* **434**, 346–353.

Kim YC, Kim SJ, Sim JH, Jun JY, Kang TM, Suh SH, So I & Kim KW (1998). Protein kinase C mediates the desensitization of CCh-activated nonselective cationic current in guinea-pig gastric myocytes. *Pflugers Arch* **436**, 1–8.

Kiselyov K, Xu X, Mozhayeva G, Kuo T, Pessah I, Mignery G, Zhu X, Birnbaumer L & Muallem S (1998). Functional interaction between $InsP_3$ receptors and store-operated Htrp3 channels. *Nature* **396**, 478–482.

Kuriyama H, Kitamura K, Itoh T & Inoue R (1998). Physiological features of visceral smooth muscle cells, with special reference to receptors and ion channels. *Physiol Rev* **78**, 811–920.

Large WA (2002). Receptor-operated Ca^{2+}-permeable nonselective cation channels in vascular smooth muscle: a physiologic perspective. *J Cardiovasc Electrophysiol* **13**, 493–501.

Levitan IB (1999). It is calmodulin after all! Mediator of the calcium modulation of multiple ion channels. *Neuron* **22**, 645–648.

Minke B & Cook B (2002). TRP channel proteins and signal transduction. *Physiol Rev* **82**, 429–472.

Montell C (2001). Physiology, phylogeny, and functions of the TRP superfamily of cation channels. *Sci STKE*. www.stke.org/cgi/content/full/OC_sigtrans; 2001/90/re1, pp. 1–17.

Mori Y, Takada N, Okada T, Wakamori M, Imoto K, Wanifuchi H, Oka H, Oba A, Ikenaka K & Kurosaki T (1998). Differential distribution of TRP Ca^{2+} channel isoforms in mouse brain. *Neuroreport* **9**, 507–515.

Okada T, Inoue R, Yamazaki K, Maeda A, Kurosaki T, Yamakuni T, Tanaka I, Shimizu S, Ikenaka K, Imoto K & Mori Y (1999). Molecular and functional characterization of a novel mouse transient recepotr potential protein homologue TRP7. *J Biol Chem* **274**, 27359–27370.

Okada T, Shimizu S, Wakamori M, Maeda A, Kurosaki T, Takada N, Imoto K & Mori Y (1998). Molecular cloning and functional characterization of a novel receptor-activated TRP Ca^{2+} channel from mouse brain. *J Biol Chem* **273**, 10279–10287.

Pacaud P & Bolton TB (1991). Relation between muscarinic receptor cationic current and internal calcium in guinea-pig jejunal smooth muscle cells. *J Physiol* **441**, 477–499.

Rusnak F & Mertz P (2000). Calcineurin: Form and function. *Physiol Rev* **80**, 1483–1521.

Saimi Y & Kung C (2002). Calmodulin as an ion channel subunit. *Annu Rev Physiol* **64**, 289–311.

Shi J, Inoue R, Mori E, Mori Y & Ito Y (2003). Contrasting nature of calcium regulation via calmodulin (CaM) for two murine transient receptor potential protein homologues TRPC6 and TRPC7. *J Pharmacol Sci* **91** (Sup I), 95P.

Siemen D (1993). Nonselective cation channels. In *Nonselective Cation Channels. Pharmacology, Physiology and Biophysics*, ed.Siemen D & Hescheler J. Birkhaeuser, Basel, Boston, Berlin.

Singh BB, Liu X, Tang J, Zhu MX & Ambudkar IS (2002). Calmodulin regulates Ca^{2+}-dependent feedback inhibition of store-operated Ca^{2+} influx by interaction with a site in the C terminus of TrpC1. *Mol Cell* **9**, 739–750.

Strübing C, Krapivinsky G, Krapivinsky L & Clapham DE (2003). Formation of novel TRPC channels by complex subunit interactions in embryonic brain. *J Biol Chem* **278**, 39014–39019.

Tang J, Lin Y, Zhang Z, Tikunova S, Birnbaumer L & Zhu MX (2001). Identification of common binding sites for calmodulin and inositol 1,4,5-trisphosphate receptors on the carboxyl termini of Trp channels. *J Biol Chem* **276**, 21303–21310.

Trebak M, Vazquez G, St Bird G, J & Putney JW Jr (2003). The TRPC3/6/7 subfamily of cation channels. *Cell Calcium* **33**, 451–461.

Vaca L & Sampieri A (2002). Calmodulin modulates the delay period between release of calcium from internal stores and activation of calcium influx via endogenous TRP1 channels. *J Biol Chem* **277**, 42178–42187.

Welsh DG, Morielli AD, Nelson MT & Brayden JE (2002). Transient receptor potential channels regulate myogenic tone of resistance arteries. *Circ Res* **90**, 248–250.

Yamada H, Wakamori M, Hara Y, Takahashi Y, Konishi K, Imoto K & Mori Y (2000). Spontaneous single-channel activity of neuronal TRP5 channel recombinantly expressed in HEK293 cells. *Neurosci Lett* **285**, 111–114.

Zhang Z, Tang J, Tikunova S, Johnson JD, Chen Z, Qin N, Dietrich A, Stefani E, Birnbaumer L & Zhu MX (2001). Activation of Trp3 by inositol 1,4,5-trisphosphate receptors through displacement of inhibitory calmodulin from a common binding domain. *Proc Natl Acad Sci U S A* **98**, 3168–3173.

Zholos AV, Tsvilovskyy VV & Bolton TB (2003). Muscarinic cholinergic excitation of smooth muscle: signal transduction and single cationic channel properties. *Neurophysiol* **35**, 311–329.

Zitt C, Obukhov AG, Strübing C, Zobel A, Kalkbrenner F, Lückhoff A & Schultz G (1997). Expression of TRPC3 in chinese hamster ovary cells results in calcium-activated cation currents not related to store depletion. *J Cell Biol* **138**, 1333– 1341.

Acknowledgements

We thank Miss Yoko Takashiro for expert technical assistance. This study is supported in part by a grant-in-aid from the Ministry of Education, Culture and Science to R.I. J.S. is a fellow of the Tokyo Biochemical Research Foundation and supported by the National Natural Science Foundation of China (grant No. 30400154).

Supplementary material

The online version of this paper can be accessed at: DOI: 10.1113/jphysiol.2004.075051 http://jp.physoc.org/cgi/content/full/jphysiol.2004.075051/DC1 and contains supplementary material consisting of three figures:

Supplementary Figure 1. Effects of Ca_o^{2+} on TRPC6/7 chimeras

Supplementary Figure 2. C-terminus determines the pattern of Ca_i^{2+} response

Supplementary Figure 3. CLUSTALW amino acid alignments of putative TM5–6 linker region between TRPC7, 6 and 5 channels.

This material can also be found at:
http://www.blackwellpublishing.com/products/journals/suppmat/tjp/tjp575/tjp575sm.htm